



ELSEVIER

Contents lists available at [SciVerse ScienceDirect](http://www.sciencedirect.com)

Comptes Rendus Physique

www.sciencedirect.com

Physics: Surfaces, interfaces, films

Hybrid organic–inorganic of ZnS embedded PVP nanocomposite film for photoluminescent application

*Nanocomposite hybride organique–inorganique de ZnS embarqué dans PVP pour l'application photoluminescente*S. Ummartyotin^a, N. Bunnak^a, J. Juntaro^b, M. Sain^b, H. Manuspiya^{a,*}^a The Petroleum and Petrochemical College, Centre of Excellence on Petrochemical and Materials Technology, Chulalongkorn University, Bangkok, 10330, Thailand^b Centre for Biocomposites and Biomaterials Processing, Faculty of Forestry, University of Toronto, 33 Willcocks Street, Toronto, M5S 3B3, Canada

ARTICLE INFO

Article history:

Received 26 March 2012

Accepted after revision 27 September 2012

Available online 6 November 2012

Presented by Jacques Villain

Keywords:

Hybrid organic–inorganic

ZnS embedded PVP

Photoluminescence

Organic light emitting diodes (OLEDs)

Mots-clés:

Le matériau composite hybride

ZnS assemble par PVP

Photoluminescence

Diode électroluminescente organique

(OLED)

ABSTRACT

ZnS nanoparticles were successfully synthesised by the wet chemical synthetic route. In order to use ZnS nanoparticles with more efficiency, a hybrid organic–inorganic ZnS embedded PVP film was consequently prepared and deposited by a desktop inkjet printer. This hybrid material exhibited blue fluorescence at the cluster of ZnS nanoparticles embedded the PVP. The photoluminescence peak located at 428 nm in the spectra excited 310 nm wavelengths. The hybrid film can be used as an emitter layer in organic light emitting diodes (OLEDs).

© 2012 Académie des sciences. Published by Elsevier Masson SAS. All rights reserved.

R É S U M É

Nanoparticules ZnS ont été bien synthétisées avec succès par voie chimique. Le composite hybride organique–inorganique de ZnS embarqué dans le film PVP a été déposé courant par imprimante à jet d'encre du bureau afin d'améliorer les propriétés d'usage. Ce matériau hybride expose la fluorescence bleue au cluster de nanoparticules ZnS embarquées dans PVP. Le pic photoluminescent a lieu à 428 nm dans les spectres sollicités à longueur d'onde de 310 nm. Le film hybride peut être utilisé en tant de la couche d'émetteur pour Diodes électroluminescentes organiques (OLEDs).

© 2012 Académie des sciences. Published by Elsevier Masson SAS. All rights reserved.

1. Introduction

Advances in research are dependent on the possibility of having different properties in the same material, ranging from an optimized processing step, excellent micro- or nano-scale structure, along with the functionalities required for the specific desired application. In recent years, many groups of researchers have successfully prepared nanocomposite systems by incorporating inorganic nanoparticles into an organic matrix [1–4]. These hybrid nanocomposites provide a path for a novel class of materials which inherits properties of both the inorganic nanoparticles and the organic matrix in order to tailor excellence in chemical and physical properties. These include mechanical strength, chemical resistance, thermal stability, as well as optical properties [5].

* Corresponding author.

E-mail addresses: m.sain@utoronto.ca (M. Sain), hathaikarn.m@chula.ac.th (H. Manuspiya).

In particular, a typical hybrid material was contained as an organic phase, bound with inorganic nanoparticles. Polyvinylpyrrolidone (PVP) is a class of organic compounds that has a well-defined structure with an *N*-vinylpyrrolidone monomer connected as a long chain. The incorporation of inorganic nanoparticles into a polymer matrix can result in significant improvements in a variety of chemical and physical properties [6,7].

On the other hand, in the case of inorganic materials, ZnS nanoparticles have been widely used as transparent electrodes in solar cells [8,9], thin film transistors [10], as well as a blue light emitter [11–13]. The most important characteristic of this nanoparticle is the exciton binding energy of ZnS. Chen et al. reported that the exciton binding energy of ZnS is 39 meV. Due to this energy band gap, the exciton is stable at ambient temperature even in a bulk particle. Owing to these properties, ZnS is an excellent candidate for optoelectronic devices such as light emitting diodes.

In our previous work, ZnS and related metal (Mn, Cu)-substituted ZnS were successfully synthesized by a wet chemical synthetic route at room temperature [14]. The reaction of zinc acetate and sodium sulfide was conducted in water. The advantages of this synthetic route are a high yield of product and relatively low energy costs. Nevertheless, ZnS and the related metal (Mn, Cu)-substituted ZnS colloid exhibited agglomeration among particles due to the existence of water. Bulk particles of ZnS and metal (Mn, Cu)-substituted ZnS can generate PL intensity, however, the use of these particles is limited due to the device fabrication process. The use of the inkjet printing technique, a commercially available method of fabricating light emitting devices, has been widely employed in market [15,16]. The use of printed nanoparticles has the limitation of particle size less than 200 nm, suggested by the supplier. To quantify the ZnS nanoparticle growth (less than 200 nm), size measurements of quantum dots are necessary. A potential protective material is the organic matrix that includes polyvinylpyrrolidone (PVP) in order to control the effective size and size distribution, but maintain the photoluminescent properties.

In this research work, we wish to extend our previous experiment. A flexible substrate was successfully prepared [17]. ZnS and metal (Mn, Cu)-doped ZnS were consequently developed. Moreover, in order to scale up this concept to commercially available material in a market using the process of continuous fabrication, an inkjet printer was widely employed. Therefore, the hybrid organic–inorganic ZnS embedded PVP was further investigated, including the possibility of using this as an emissive layer on OLED devices with higher efficiency.

2. Experimental

2.1. Chemical reagents

Sodium sulfide ($\text{Na}_2\text{S}\cdot 9\text{H}_2\text{O}$) and zinc sulfate ($\text{ZnSO}_4\cdot 7\text{H}_2\text{O}$) were purchased from Caledon Chemical Company, Canada and J.T. Baker Chemical Company, Canada, respectively. Polyvinylpyrrolidone (PVP) ($M_w \sim 10\,000$) was purchased from Sigma Aldrich Company, Canada. Analytical grade of methanol was purchased from Bioshop, Canada. Distilled water and analytical grade of methanol were used as solvents. All the chemical reagents were used without further purification.

2.2. Instruments

2.2.1. Fourier transform infrared spectroscopy

FTIR was performed on a Bruker Vector 22 mid-IR spectroscopy (Bruker, Germany). All FTIR absorption spectra were recorded over the $4500\text{--}500\text{ cm}^{-1}$ wavenumber region at a resolution of 8 cm^{-1} with 1024 scans using a deuterated triglycine sulfate (DTGS) detector. A straight line between the two lowest points in the respective spectra region was chosen as a baseline. Potassium bromide (KBr) acting as a non-absorbing medium was mixed with a solid sample (0.3–0.5 wt%) by an agate mortar and pestle to prepare a pellet specimen.

2.2.2. X-ray diffraction

The synthesized ceramic powders were stored in an oven at above 150°C overnight for water absorption prevention. The crystal structure of the powders was analyzed by XRD (Phillips P.W. 1830 diffractometer) using nickel-filtered $\text{Cu-K}\alpha$ radiation. Diffraction patterns were recorded over a range of $25\text{--}80^\circ$. The consistency result was compared with literature.

2.2.3. Scanning electron microscope and energy dispersive analysis

The powders were investigated by SEM (a JOEL JSM-6301F scanning microscope). The machine was operated at an acceleration voltage of 20 keV at a working distance of 15 mm to identify the morphological properties of powders. Before investigation, the samples were sputter-coated with Au to enhance the electrical conductivity.

2.2.4. Laser confocal microscope and photoluminescence spectroscopy

Laser confocal microscope and luminescence experiments were performed using an Olympus BX41 fiber-coupled confocal microscope. Excitation of the dopant ions is performed using a continuous argon laser. The excitation beam was focused on the sample surface by means of a 100 achromatic microscope objective (NA0.9) down to approximately 0.3 mm spotsize. To separate the excitation beam and the sample luminescence, an interference filter that removes the excitation wavelength (notch filter) was used. The fluorescence was focused into a fiber-coupled high-resolution spectrometer (SPEX500M) and then detected using a CCD camera.

2.2.5. Transmission electron microscope

The particle size of ZnS was investigated by TEM, Hitachi H-7000. The ZnS solution was suspended in methanol and dropped on a molybdenum grid. After, the grid was dried at 50 °C for methanol evaporation and kept into the TEM chamber. The image thus obtained was processed with computer for identification of the domains in which certain lattice fringes appear. For this propose, TEM image was captured at 40 000× magnification. The acceleration voltage of electron beam was set at 75 keV.

2.2.6. Desktop inkjet printer

The Dimatix DMP-2800 inkjet printer (Fujifilm Dimatix, Inc., Santa Clara, CA, USA) was used to deposit conductive solution on a 50 × 50 mm² substrate with a disposable piezo inkjet cartridge. The cartridge reservoir contained 2 ml of ZnS/PVP solution. The temperature of vacuum plate, which secured the substrate in place, was adjusted to 60 °C.

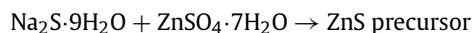
ZnS/PVP solution was filtered by a nano-size filter (200 nm) before usage in order to prevent agglomeration among silver particles and to control the ink particle size (< 200 nm), suggesting by desktop inkjet supplier.

2.3. Methods

2.3.1. Preparation of ZnS nanoparticle

The ZnS nanoparticles were prepared as follows: 10 g of Na₂S·9H₂O were added to 50 ml of distilled water. The mixture was stirred for 1 hour. In parallel, 10 g of ZnSO₄·7H₂O were also dissolved into 50 ml of distilled water. Na₂S·9H₂O solution was then poured into the ZnSO₄·7H₂O solution.

The stoichiometric of chemical reaction is as follows:



After, 10 g of PVP were subsequently added into the ZnS precursor solution. The reaction was continuously stirred for 3 hours at room temperature. Then, the solution was centrifuged at 500 rpm for 30 min in order to remove the solvent. The obtained ZnS nanoparticles would precipitate.

2.3.2. Preparation of ZnS embedded PVP as a hybrid nanocomposite film

The ZnS/PVP solution was dissolved in 3 ml of water and loaded into the cartridge reservoir of the desktop inkjet printer. Each of 3 ink formulations was sonicated for 3 hours prior to printing in order to prevent the agglomeration among ink particles. Then, the amount of solution and plate temperature was controlled at 3 ml and 50 °C. After that, the deposited-silver film was dried at 180 °C overnight.

3. Results and discussion

ZnS nanoparticles were successfully synthesized by the wet chemical synthetic route. The ZnS solution exhibited a milky-white color. The viscosity, measured by Ubbelohde type canon, was 14 cgs. It was thus acceptable for usage of desktop inkjet printer. The range of viscosity should be in 10–20 cgs at room temperature, suggested by the inkjet printer supplier. In addition, this technique of synthesis effectively offered a high yield of the product and excellent colloidal stability. In this synthetic procedure, polyvinylpyrrolidone (PVP) was chosen as the stabilizer for forming the precursor of ZnS. It can offer the ZnS nanoparticles exposure to the carboxylic functionality of PVP to the outer environment, leading to a very hydrophilic surface which makes the ZnS stable in water.

However, the limitation of as-synthesized ZnS exhibited agglomeration among the nanoparticles; the preferable use of this particle must be less than 200 nm. In order to prevent this phenomenon, the other role of PVP is used to control and stabilize the particle size of ZnS. Therefore, we developed an analogous procedure for making the as-synthesized ZnS as a hybrid nanocomposite film.

The absorption FTIR spectra of the ZnS/PVP solution and ZnS/PVP hybrid nanocomposite film were recorded in the range of 4000 to 500 cm⁻¹ and are exhibited in Fig. 1. In the case of the ZnS/PVP hybrid nanocomposite film, the peaks appearing at 1200 and 620 cm⁻¹ are due to Zn–S vibration and at 2920, 2360 and 1640 cm⁻¹ are due to microstructure formation of the sample. On the other hand, this is in contrast to the ZnS/PVP solution, the peak appearing from 1200 to 500 cm⁻¹ was featureless. This is due to the small amount of ZnS nanoparticles in solution. However, the broad absorption peak in the range of 3410–3465 cm⁻¹ corresponding to –OH group indicated the existence of water absorbed in the surface of the nanoparticles. The presence of this band can be clearly attributed to the adsorption of same atmospheric water during measurement. The bands at 1600 and 2370 cm⁻¹ are due to the C–O stretching modes arising from the absorption of atmospheric CO₂ on the surface. All of the appearing peak values are in good agreement with the previous literature [18,19].

The XRD patterns of the neat PVP film, ZnS embedded PVP film and bulk ZnS are exhibited in Fig. 2. X-ray diffraction technique was used to investigate the crystalline structure of film materials. No diffraction peak was detected for the neat PVP film, suggesting that it did not contain any crystallite structure. However, more diffraction peaks appeared in the case of the ZnS embedded PVP film. Three positions can be remarkably corresponded to the lattice planes of (111), (220) and (311), are very well matched with the cubic ZnS structure (JCPDS No. 05-0566). This result is consistent with bulk ZnS [20].

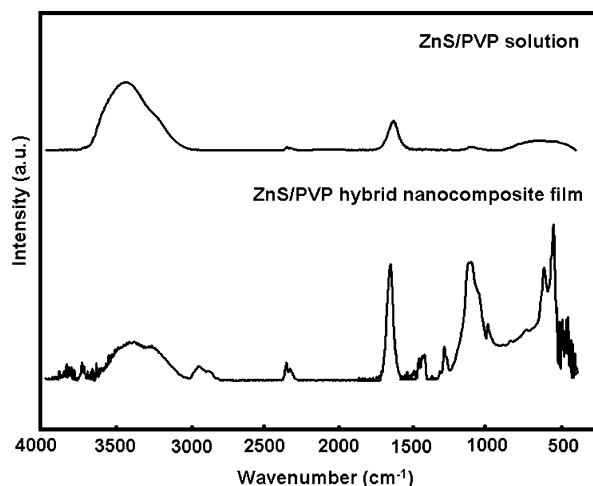


Fig. 1. FTIR spectra of ZnS/PVP solution and ZnS/PVP hybrid nanocomposite film.

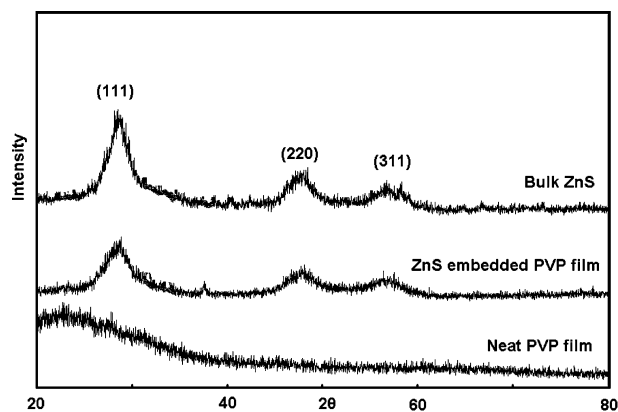


Fig. 2. XRD spectra of neat PVP film, ZnS embedded PVP film and bulk ZnS particles.

According to the Debye–Scherrer formula, the mean crystallite sizes calculated from the full width at half maximum (FWHM) are:

$$D = k\lambda / (\beta \cos \theta)$$

where D is the mean grain size, k is a constant (the shape factor, approximately 1), λ is the X-ray wavelength (1.54056 Å for Cu-K α), β is the full width at half maximum (FWHM) of the diffraction peak and θ is the Bragg angle.

According to the FWHM of the most intense peak (111) plane, the average crystallite size of ZnS was 50 Å. This is close to the value deduced from SEM and TEM imaging.

The TEM and SEM micrographs of the ZnS nanoparticles are given in Figs. 3(A) and 3(B), respectively. The particle size was estimated with the distribution histogram that exhibited the maximum frequency for the states particle range. The shape of the nanoparticles exhibited spherical form, and the size was about 30–50 Å. A comparison of particle sizes obtained XRD and TEM illustrated good agreement. On the other hand, the SEM image exhibited an agglomeration character among nanoparticles due to solvent removal. Three points on the SEM image show the position of EDX analysis. This revealed that the amount of zinc and sulfur atoms can be detected.

Fig. 4 shows that ZnS embedded PVP was successfully deposited on our substrate. The SEM image revealed that the morphology of the deposited film has uniform surface. The inkjet printer offered a printed film with high density on the printed area. No space can be observed. The ZnS nanoparticles had successfully penetrated the surrounding PVP matrix. The presence of white color represented the position of ZnS nanoparticles. The homogeneous distribution of ZnS was successfully controlled by the use of sonicator on the ink solution prior to printing. However, the film still exhibited a crack-like character. Before SEM observation, the hybrid ZnS embedded PVP was deposited on a flexible substrate. The optimization between mechanical properties and expected device efficiency need to be considered in order to prevent crack phenomena.

On the other hand, the insert in Fig. 4 exhibits the EDX analysis. It shows that the deposited film was mainly composed of zinc and sulfur atoms within the scan area (pink color). The presence of carbon and oxygen was possibly due to the use of carbon tape and retained solvent after the deposition step.

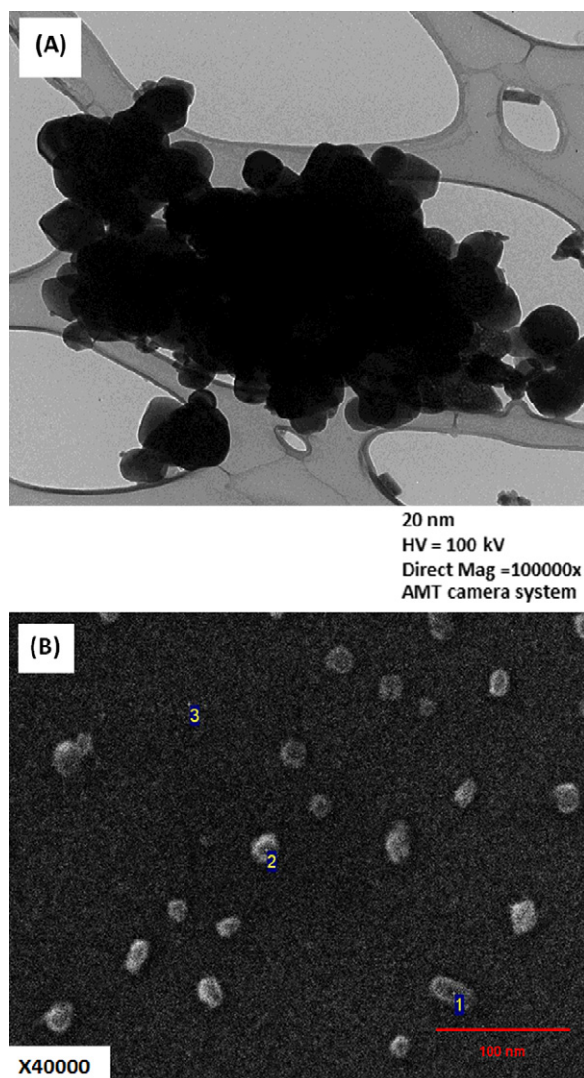


Fig. 3. TEM (A) and SEM (B) image of ZnS nanoparticles.

After, the printed hybrid organic–inorganic ZnS embedded PVP film was observed by laser confocal microscope. Fig. 5(A) shows a fluorescence image of ZnS nanoparticles without excitation, where numerous ZnS clusters were aggregated from smaller particles. Under excitation of an UV light of 320 nm, they emit strong blue fluorescence light as exhibited in Fig. 5(B). The blue color corresponds to those clusters. On the other hand, the photoluminescence spectrum in Fig. 6 exhibits a PL at 428 nm excited with 310 nm wavelength, completely coinciding with the blue fluorescence light. However, the intensity of PL spectrum was still low; no sharp peak can be detected. This is probably due to complete covering of ZnS on PVP matrix.

4. Conclusion

ZnS nanoparticles were synthesized by a wet chemical synthetic route. A hybrid organic–inorganic ZnS embedded PVP film was consequently deposited on a substrate by a desktop inkjet printer. The film emitted a blue fluorescence from the ZnS clusters which penetrated among the PVP matrix. This hybrid material can be used as an emitter layer in organic light emitting diodes (OLEDs).

Acknowledgements

The authors would like to thank ABIP, NSERC Manufacturing Network and CG Tower for their financial support. Partially financial support from Thailand Government Research budget no. GRB_BSC_54_55_6_07 was acknowledged. The use of laser confocal and transmission electron microscope at Centre for Nanostructure Image, Department of Chemistry, University of Toronto is appreciated. The authors also extend their appreciation to the Center of Excellence for Petroleum, Petrochemicals and Advanced Materials, Chulalongkorn University for scholarship (for S.U.).

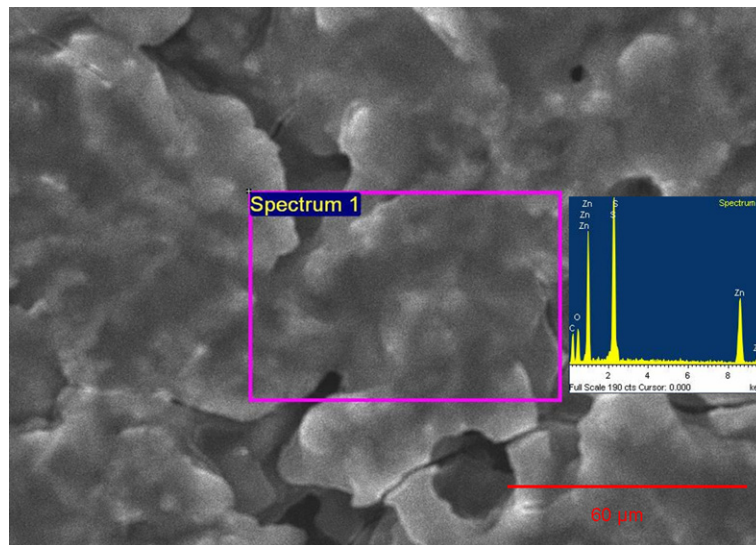


Fig. 4. SEM image of printed hybrid organic–inorganic ZnS embedded PVP film. (For interpretation of the references to color in this figure, the reader is referred to the web version of this article.)

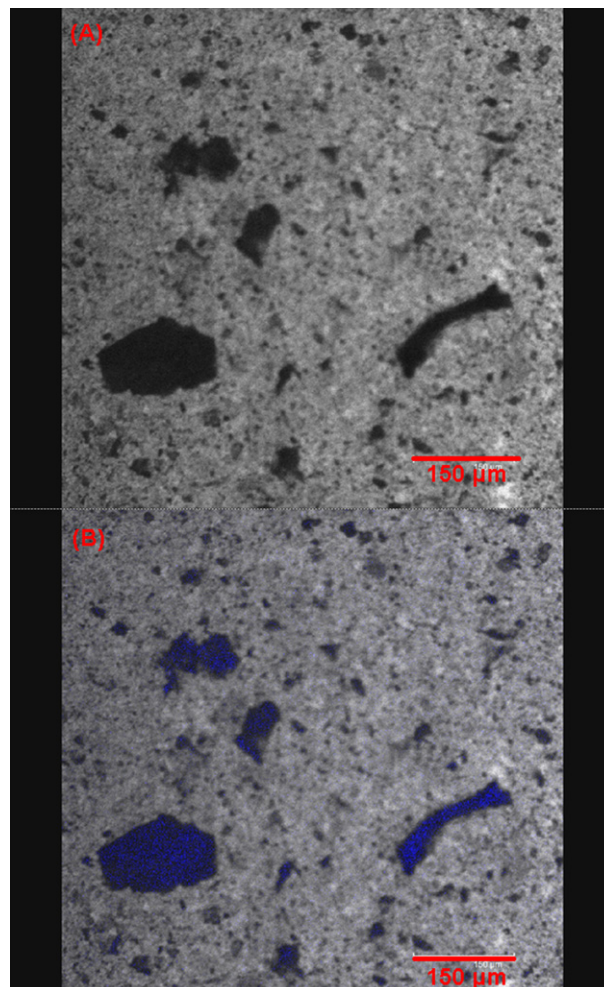


Fig. 5. Photoluminescent image of ZnS embedded nanocomposite (A) without excitation, (B) with excitation. (For interpretation of the references to color in this figure, the reader is referred to the web version of this article.)



Fig. 6. PL spectra of ZnS embedded PVP hybrid nanocomposite.

References

- [1] D.M. Fernandes, et al., Preparation, characterization, and photoluminescence study of PVA/ZnO nanocomposite films, *Materials Chemistry and Physics* 128 (2011) 371–376.
- [2] Y. Feng, et al., Synthesis and characterization of luminescent organic–inorganic hybrid nanocomposite from polyhedral oligomeric silsesquioxane, *Chinese Chemical Letters* 21 (2010) 753–757.
- [3] P.K. Khanna, N. Singh, Light emitting CdS quantum dots in PMMA: Synthesis and optical studies, *Journal of Luminescence* 127 (2007) 474–482.
- [4] J.G. Liu, et al., Facile synthesis and characterization of CdTe quantum dots–polystyrene fluorescent composite nanospheres, *Materials Letters* 63 (2009) 2224–2226.
- [5] A. Antonello, et al., Hybrid organic–inorganic ZnS-loaded nanocomposite films for stable optical coatings, *Thin Solid Films* 518 (2010) 6781–6786.
- [6] T. Du, H. Song, O.J. Ilegbusi, Sol–gel derived ZnO/PVP nanocomposite thin film for superoxide radical sensor, *Materials Science and Engineering C* 27 (2007) 414–420.
- [7] O.J. Ilegbusi, H. Song, R. Chakrabarti, Biocompatibility and conductometric property of sol–gel derived ZnO/PVP biosensors film, *Journal of Bionic Engineering* 7 (2010) 30–35.
- [8] T. Nakada, M. Hongo, E. Hayashi, Band offset of high efficiency CBD-ZnS/CIGS thin film solar cells, *Thin Solid Films* 431–432 (2003) 242–248.
- [9] I.O. Oladeji, L. Chow, Synthesis and processing of CdS/ZnS multilayer films for solar cell application, *Thin Solid Films* 474 (2005) 77–83.
- [10] Z.H. Chen, et al., Epitaxial ZnS/Si core–shell nanowires and single-crystal silicon tube field-effect transistors, *Journal of Crystal Growth* 310 (2008) 165–170.
- [11] J.M. Hwang, et al., Preparation and characterization of ZnS based nano-crystalline particles for polymer light-emitting diodes, *Current Applied Physics* 5 (2005) 31–34.
- [12] C.W. Lee, et al., Investigations of organic light emitting diodes with CdSe(ZnS) quantum dots, *Materials Science and Engineering B* 147 (2008) 307–311.
- [13] H. Cho, et al., Highly flexible organic light-emitting diodes based on ZnS/Ag/WO₃ multilayer transparent electrodes, *Organic Electronics* 10 (2009) 1163–1169.
- [14] S. Ummartyotin, et al., Synthesis and luminescence properties of ZnS and metal (Mn, Cu)-doped-ZnS ceramic powder, *Solid State Sciences* 14 (2012) 299–304.
- [15] Y. Yoshioka, G.E. Jabbour, Desktop inkjet printer as a tool to print conducting polymers, *Synthetic Metals* 156 (2006) 779–783.
- [16] H. Cho, M. Parameswaran, H.Z. Yu, Fabrication and microsensors using unmodified office inkjet printers, *Sensors and Actuators B: Chemical* 123 (2007) 749–756.
- [17] S. Ummartyotin, et al., Development of transparent bacterial cellulose nanocomposite film as substrate for flexible organic light emitting diode (OLED) display, *Industrial Crops and Products* 35 (2012) 92–97.
- [18] Y.Y. She, J. Yang, K.Q. Qiu, Synthesis of ZnS nanoparticles by solid–liquid chemical reaction with ZnO and Na₂S under ultrasonic, *Transaction Nonferrous Metal Society of China* 20 (2010) 211–215.
- [19] J.S. Jang, et al., Topotactic synthesis of mesoporous ZnS and ZnO nanoplates and their photocatalytic activity, *Journal of Catalysis* 254 (2008) 144–155.
- [20] C. Chlique, et al., A comparative study of ZnS powders sintering by hot uniaxial pressing (HUP) and spark plasma sintering (SPS), *Optical Materials* 33 (2011) 706–712.